Numerical Monte Carlo analysis of the influence of pore-scale dispersion on macrodispersion in 2-D heterogeneous porous media

Anthony Beaudoin, Jean-Raynald de Dreuzy, Jocelyne Erhel

Numerical Monte Carlo analysis of the influence of pore-scale dispersion on macrodispersion in 2-D heterogeneous porous media

Anthony Beaudoin,[1,2] Jean-Raynald de Dreuzy,[3,4] and Jocelyne Erhel[5]

Received 21 May 2010; revised 6 September 2010; accepted 20 September 2010; published 14 December 2010.

[1] We investigate the influences of pore-scale dispersion and of larger-scale permeability heterogeneities on the macrodispersion without the molecular diffusion. Permeability follows a lognormal exponentially correlated distribution characterized by its correlation length λ and its lognormal variance σ^2. Macrodispersion is evaluated numerically by using parallel simulations on grids of characteristic size ranging from 200λ to 1600λ. We note α_L and α_T the pore-scale longitudinal and transversal dispersivities. For $\alpha_L/\lambda < 10^{-2}$ and $\alpha_T/\lambda < 10^{-3}$, the influence of pore-scale dispersion on the macrodispersion is smaller than 5% of the macrodispersion due only to permeability heterogeneities. Larger dispersivities ($\alpha_L/\lambda \geq 10^{-2}$ or $\alpha_T/\lambda \geq 10^{-3}$) induce larger effects than those obtained by the semianalytical expression of Salandin and Fiorotto (1998) for $\sigma^2 > 1$. The effects of local dispersion on the longitudinal macrodispersion remain limited to 25% at most of the macrodispersion due only to permeability heterogeneities. For $\sigma^2 > 1$, isotropic local dispersion induces a reduction of the longitudinal macrodispersion, whereas anisotropic local dispersion lets it increase. The longitudinal and transverse local dispersions induce opposite effects on the longitudinal macrodispersion, which are respectively an increase and a reduction. The transverse macrodispersion null without local dispersion or molecular diffusion becomes strictly positive with local dispersion. Because of the velocity field heterogeneities, it is amplified by a factor of 2 to 50 from the grid scale to the macro scale. The transverse dispersion is triggered by both longitudinal and transverse local dispersions. A reduction of a factor of 2 of the transverse local dispersion at fixed longitudinal local dispersion yields only a reduction of a factor of 4 at most of the transverse macrodispersion for $\sigma^2 \geq 2.25$.

Citation: Beaudoin, A., J.-R. de Dreuzy, and J. Erhel (2010), Numerical Monte Carlo analysis of the influence of pore-scale dispersion on macrodispersion in 2-D heterogeneous porous media, *Water Resour. Res.*, *46*, W12537, doi:10.1029/2010WR009576.

1. Introduction

[2] Field-scale dispersion results from the variations in fluid velocity occurring from the pore scale to the formation scale and from molecular diffusion [*Frippiat and Holeyman*, 2008; *Gelhar et al.*, 1992]. It is modeled by an equivalent diffusion law parameterized by the dispersion tensor D [*Bear*, 1973]. Its components are given by

$$D_{ij} = (\alpha_T|v| + d)\delta_{ij} + (\alpha_L - \alpha_T)\frac{v_i v_j}{|v|}, \quad (1)$$

where α_L and α_T are the longitudinal and transverse dispersivities, respectively, d is the molecular diffusivity, v is the fluid velocity, and δ_{ij} is the Kronecker delta function. This formalism is mostly used at two scales. At the local scale, the dispersion coefficient results from the effects of the variations of the pore-scale fluid velocity. At field scale, the dispersion coefficient, also called the macrodispersion coefficient, comes both from the previous local effects and from the variations in fluid velocities due to permeability heterogeneities. In this study, we focus on the effects of the local dispersion on the macrodispersion coefficient for highly heterogeneous two-dimensional (2-D) porous media. We take the most classical model in the context of porous media. It consists of an exponentially correlated lognormal isotropic permeability field [*Freeze*, 1975; *Gelhar*, 1993]. It is characterized by the variance of the distribution of the logarithm of the permeability σ^2 and by its correlation length λ. Its correlation function is given by

$$C(r) = \sigma^2 \exp\left(-\frac{|r|}{\lambda}\right), \quad (2)$$

where r is the vector between two points. The originality of this work does not rely on the correlation structure but on the magnitude of the heterogeneity. We investigate high-heterogeneity cases for which $\sigma^2 \in [1, 9]$, while most

[1]LOMC, Université du Havre, Le Havre, France.
[2]Institut P′, UPR 3346 CNRS, Université de Poitiers, ENSMA, SP2MI, Chasseneuil, France.
[3]Géosciences de Rennes, UMR 6118 CNRS, Université de Rennes 1, Campus de Beaulieu, Rennes, France.
[4]Institute of Environmental Assessment and Water Research, CSIC, Barcelona, Spain.
[5]INRIA, Campus de Beaulieu, Rennes, France.

0043-1397/10/2010WR009576

previous studies dealt with the low heterogeneity cases ($\sigma^2 < 1$) [*Chaudhuri and Sekhar*, 2005; *Fiori*, 1996, 1998; *Gelhar and Axness*, 1983]. High and low heterogeneity cases can lead to fundamentally different behaviors [*de Dreuzy et al.*, 2007; *Dentz and Tartakovsky*, 2008; *Jankovic et al.*, 2003]. For example, for 2-D pure advection cases, while it has been well established that the longitudinal macrodispersion coefficient depends linearly on σ^2 for low-heterogeneity cases [*Gelhar and Axness*, 1983], recent numerical and theoretical studies show that it depends on the square of σ^2 for high-heterogeneity cases [*de Dreuzy et al.*, 2007; *Dentz and Tartakovsky*, 2008]. We identify the macrodispersion coefficient with the asymptotic dispersion coefficient in these cases of lognormally finitely correlated permeability fields. In this study, even if the permeability heterogeneity is high, it is still limited ensuring the convergence of the longitudinal and transverse dispersion coefficients to finite values.

[3] For low levels of heterogeneity ($\sigma^2 < 1$) and local dispersivities much smaller than the correlation length ($\alpha_L \ll \lambda$ and $\alpha_T \ll \lambda$), the first-order perturbation analysis of *Gelhar and Axness* [1983] shows that the local dispersion does not modify the leading order of the longitudinal macrodispersion coefficient $D_{LA}(GA)$ and lets the transverse dispersion coefficient $D_{TA}(GA)$ increase according to

$$\frac{D_{LA}(GA)}{u} = \lambda\sigma^2, \tag{3}$$

$$\frac{D_{TA}(GA)}{u} = \frac{\sigma^2}{8}(\alpha_L + 3\alpha_T), \tag{4}$$

where index A stands for asymptotic dispersion equivalent here to macrodispersion as previously said, (GA) is an identifier for the solution of *Gelhar and Axness* [1983] and u is the mean velocity. The longitudinal macrodispersion coefficient is proportional to the correlation length λ. The transverse macrodispersion coefficient is the sum of two terms proportional to the local longitudinal and transverse dispersivities, α_L and α_T, respectively. Semianalytical approaches accounting in the dispersion term for velocity variations confirm the lack of strong dependence of the longitudinal macrodispersion coefficient on σ^2 [*Salandin and Fiorotto*, 2000]. *Salandin and Fiorotto* [2000] show that the local dispersion induces an increase of both the longitudinal and transverse macrodispersion coefficients for $\sigma^2 < 1$. Differences with the solution of *Gelhar and Axness* [1983] are more important for the transverse component than for the longitudinal component of the macrodispersion.

[4] For high-heterogeneity cases ($\sigma^2 > 1$), *Salandin and Fiorotto* [2000] use their semianalytical solution to predict a decrease of the longitudinal macrodispersion coefficient. They also give an estimate of the transverse macrodispersion coefficient. Still for $\sigma^2 > 1$, the sole numerical simulations have been performed for single realizations with α_L = 0.15 m and α_T = 0.015 m on a 2047 × 511 m grid with 1 × 1 m square grid cells [*Trefry et al.*, 2003]. For λ = 2 m and 8 m corresponding to $\lambda/\alpha_L \approx 13.5$ and $\lambda/\alpha_L \approx 54$, respectively, the normalized time-dependent longitudinal dispersion coefficient $D_L(t)/(u\lambda\sigma^2)$ ranges between 1.2 and 1.4 in the first case and between 1 and 1.75 in the second case for $0.25 < \sigma^2 < 4$. No conclusion can be drawn from the time-dependent transverse dispersion coefficient $D_T(t)$ because of its high variability due to the strong influence of local fluctuations in the velocity field. The main difficulty of numerical studies comes from the necessity to perform large scale and finely resolved Monte Carlo simulations.

[5] In previous studies, we set up a methodology to determine the macrodispersion coefficient from large-scale Monte Carlo parallel numerical simulations on pure advection and advection-diffusion cases [*de Dreuzy et al.*, 2007]. We perform intensive numerical simulations to investigate the respective effects of local dispersion and of permeability fluctuations on macrodispersion for the high heterogeneity cases. After describing the methods to solve the advection-dispersion equation and to determine the macrodispersion in sections 2 and 3, we present the results and discuss them in sections 3 and 4.

2. Model, Numerical Schemes, and Algorithms

[6] We describe first the hydrogeological model and, second, the numerical methods used for obtaining the permeability field and for simulating flow and the transport processes. The methods used are classical. Their implementation has been tuned for efficiency in order to simulate large and finely resolved domains. The contribution of this paper concerns neither the model nor the numerical schemes, but rather the results of macrodispersion. We thus only recall the model assumptions, the numerical schemes, and the main convergence proofs of macrodispersion to its asymptotic regime. More detailed justifications are provided in work by *de Dreuzy et al.* [2007] and by A. Beaudoin et al., Convergence analysis of advection diffusion simulations in 2-D heterogeneous porous media, unpublished, 2010. Because the permeability field is characterized by statistical laws, the resulting modeling is stochastic. In this paper, we use a basic nonintrusive Monte Carlo method.

[7] Lognormally and exponentially correlated permeability fields are generated with a Fourier transform method [*Gutjahr*, 1989; *Pardo-Igúzquiza and Chica-Olmo*, 1993] using the parallel library FFTW [*Frigo and Johnson*, 2005]. The computation domains are regular square or rectangular grids of sizes L_x and L_y with square grid cells ($dx = dy = l_m$). The aspect ratio of the system L_x/L_y ranges from 1 to 2 in square to rectangular domains. The total number of grid cells varies between 2048 × 2048 and 16384 × 8192. The key characteristic scale is the permeability correlation length, λ, giving sense to the other scales. L_x/λ is the number of correlation length in the main flow direction taken here as x. The λ/l_m is the grid cell resolution per correlation length. Ideally L_x/λ and λ/l_m should be both as large as possible.

[8] Flows follow the classical steady-state diffusion equation $\nabla(K\nabla h) = 0$ with K the permeability and h the hydraulic head. Boundary conditions are like those on a permeameter with a fixed head on the vertical sides and no flow on the horizontal sides of the domain. The flow equations is discretized with a finite volume scheme and harmonic intermesh permeabilities [*Chavent and Roberts*, 1991]. The finite volume discretization yields a large-scale linear system solved with the algebraic multigrid method implemented in HYPRE [*Erhel et al.*, 2009; *Falgout et al.*, 2005]. Velocity is first computed on each grid face and then derived within the grid cells from linear interpolations both in x and y directions as it is the sole interpolation scheme that verifies the continuity equation [*Pollock*, 1988].

[9] Solute concentration c follows the classical advection dispersion equation with the dispersion tensor D given by equation (1) for a constant porosity,

$$\frac{\partial c}{\partial t} + \nabla \cdot (vc) - \nabla \cdot (D \cdot \nabla c) = 0, \tag{5}$$

where we recall that v is the local velocity. Injection is instantaneous on a large segment of length $I = 0.4L_y$ perpendicular to the main flow direction and centered on the domain medium line. The segment is shifted downstream from the domain inlet by a distance of λ to avoid border effects. Injection is proportional to flow. The large injection window ranging from 80 to 320 correlation lengths is designed to speed up the convergence to the asymptotic regime. The rate of advection to hydrodynamic dispersion is measured by the nondimensional Peclet numbers

$$Pe_L = \lambda/\alpha_L \quad \text{and} \quad Pe_T = \lambda/\alpha_T \tag{6}$$

in the longitudinal and transverse directions, respectively. In sections 4 and 5, we compare the advection dispersion results with previously obtained advection diffusion results at equivalent Peclet numbers. The Peclet number then characterizes the rate of advection to diffusion and is defined by

$$Pe = \lambda u/d, \tag{7}$$

where we recall that u is the mean velocity and d is the diffusion coefficient. As opposed to diffusion, which is constant in the domain, hydrodynamic dispersion is locally variable because of its dependence on velocity. The problem is different from the advection-diffusion case [*de Dreuzy et al.*, 2007]. For hydrodynamic dispersion, the local rate of advection to dispersion is constant where it is highly variable for advection to diffusion. Transport was simulated by a random walk particle tracking method fully described in several review papers [*Delay et al.*, 2005; *Hoteit et al.*, 2002; *Ramirez et al.*, 2008; *Salamon et al.*, 2006]. The random walk method solves for the following Fokker-Planck equation [*van Kampen*, 1981],

$$\frac{\partial c}{\partial t} + \nabla \cdot ((v + \nabla \cdot D)c) - \nabla\nabla : (Dc) = 0. \tag{8}$$

We use the reflection method [*La Bolle et al.*, 1996; *Uffink*, 1985] to handle the discontinuities of the dispersion gradient. This choice is however not critical as it has been shown that dispersion results are not very sensitive to the method chosen for lognormally and finitely correlated permeability fields, even for σ^2 values as large as 4 [*Salamon et al.*, 2006]. Particles are injected according to flow in the injection window and are tracked using a parallel algorithm with synchronized communications of particles between CPUs [*Beaudoin et al.*, 2007].

[10] Our results rely on the effective dispersion coefficient [*Dentz et al.*, 2000; *Kitanidis*, 1988]. In the preasymptotic regime, the effective dispersion differs from the ensemble dispersion. The effective dispersion coefficient is obtained by averaging the dispersion coefficients obtained on a realization basis. The ensemble dispersion is defined by first averaging the moments over the simulations and second by deriving the dispersion. The ensemble dispersion is systematically larger than the effective dispersion as it measures the plume dispersion around the mean plume position computed over all simulations [*Dentz et al.*, 2000]. The choice of the effective over the ensemble dispersion is only motivated by convergence issues as both are asymptotically equal. The interest of the effective dispersion over the ensemble dispersion is to take advantage of the largest possible time span over which solute has not begun to reach the outlet of the domain. In equivalent words, the advantage of the effective dispersion is to avoid the limitations induced by the finite size of the domain and the dispersion of the breakthrough times between simulations. The longitudinal and transverse dispersion coefficients are first derived on a realization basis according to

$$D_L^i(t) = \frac{1}{2\lambda u} \frac{d\left(\langle x^2(t)\rangle_i - \langle x(t)\rangle_i^2\right)}{dt}, \tag{9}$$

$$D_T^i(t) = \frac{1}{2\alpha_T u} \frac{d\left(\langle y^2(t)\rangle_i - \langle y(t)\rangle_i^2\right)}{dt}, \tag{10}$$

respectively, where $\langle x^k(t)\rangle_i$ and $\langle y^k(t)\rangle_i$ are the kth moments of the solute plume of the ith simulation. We emphasize that the longitudinal and transverse dispersion coefficients of equations (9) and (10) are normalized by λu and $\alpha_T u$, respectively. These different normalization factors are deduced from the low heterogeneity approximations given by equations (2) and (3). In the absence of dispersion ($\alpha_L = \alpha_T = 0$), but with diffusion ($d > 0$), we normalize the transverse macrodispersion by the diffusion coefficient d. Equation (10) is replaced by

$$D_T^i(t) = \frac{1}{2d} \frac{d\left(\langle x^2(t)\rangle_i - \langle x(t)\rangle_i^2\right)}{dt}. \tag{11}$$

The average over N_S Monte Carlo simulations is performed in a second step

$$D_L(t) = \left\langle D_L^i(t)\right\rangle_{i=1,N_s} \quad \text{and} \quad D_T(t) = \left\langle D_T^i(t)\right\rangle_{i=1,N_s}. \tag{12}$$

The $\langle x^k(t)\rangle_i$ and $\langle y^k(t)\rangle_i$ are approximated from the random walker position moments computed on realization bases,

$$\langle x^k(t)\rangle_i = \frac{1}{N_p}\sum_{j=1}^{N_p}\left(x_j^i(t)\right)^k \quad \text{and} \quad \langle y^k(t)\rangle_i = \frac{1}{N_p}\sum_{j=1}^{N_p}\left(y_j^i(t)\right)^k, \tag{13}$$

where $x_j^i(t)$ and $y_j^i(t)$ are the coordinates of the jth particle within the ith simulation, N_p is the number of particles for one simulation. All time-dependent dispersion results will be presented against t_N defined as the time t normalized by the characteristic time necessary to cross a correlation length λ/u ($t_N = tu/\lambda$).

3. Convergence to the Asymptotic Regime

[11] This study summarizes the guidelines for the choice of the different numerical parameters. We have also performed a more detailed convergence analysis of the numerical methods used for simulating flow and transport (A. Beaudoin et al., Convergence analysis of advection diffusion simulations in 2-D heterogeneous porous media,

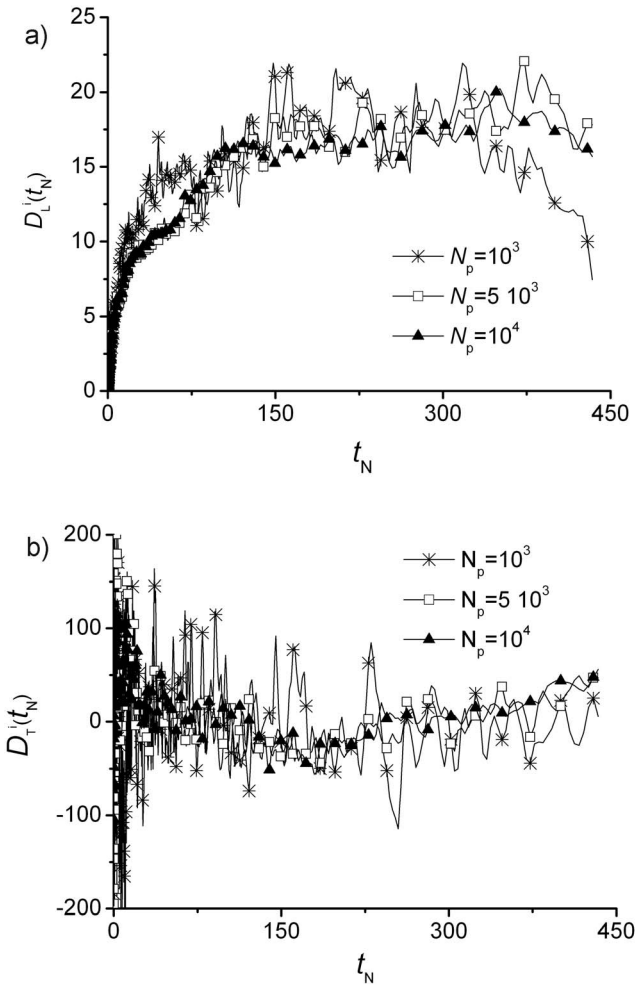

Figure 1. Normalized (a) longitudinal and (b) transverse dispersion coefficients as expressed by equations (9) and (10) for a single simulation against the normalized time for increasing particle numbers with $Pe_L = Pe_T = 20$, $d = 0$, $\sigma^2 = 9$, $\lambda/l_m = 10$ and $L_x/\lambda = L_y/\lambda = 819.2.\lambda$.

unpublished, 2010). We first handle the convergence of the time-dependent dispersion coefficients with the particle number N_p, Secondly, we study the convergence of dispersion to its asymptotic regime and determine the necessary system sizes in terms of correlation lengths L/λ.

3.1. Convergence With Particle Number N_p

[12] Previous studies have pointed out the importance to perform a statistically representative sampling of the velocity field. It is especially important for systems consisting of inclusions [*Fiori et al.*, 2008]. For the heterogeneous grids considered here, we have shown that, for the pure advection cases, 5000 particles were enough [*de Dreuzy et al.*, 2007; *de Dreuzy et al.*, 2008]. Figure 1 shows the longitudinal and transverse time-dependent dispersion coefficients $D_L^i(t)$ and $D_T^i(t)$, respectively, for a single realization taken with the largest variance $\sigma^2 = 9$ and a particle number N_p evolving from 1000 to 10,000. From $N_p = 1000$ to $N_p = 5000$, both the longitudinal and transverse dispersions are significantly modified with a decrease of their variability and more discernable asymptotic tendencies. From $N_p = 5000$ to $N_p = 10{,}000$, some differences remain but it does not change the asymptotic behavior. For the simulations presented on Figure 1, the differences between the averages of the time-dependent dispersion coefficients for t_N in the interval [200, 400] are limited to 4% and 8% for the longitudinal and transverse dispersion coefficients, respectively. We also note that there is no systematic increase of the dispersion coefficients with the number of particles even when increasing it from 1000 to 10,000. This shows that 5000 particles are enough for a statistically representative sampling of the velocity field. As the largest σ^2 case is the most detrimental one, the particle number N_p is fixed to 5000 for all simulations. Given that the injection segment length varies between 80λ and 320λ, the initial sampling of the permeability field corresponds to 15 to 60 particles per correlation length on average.

3.2. Convergence With the Domain Size in Terms of Correlation Lengths

[13] The convergence of the macrodispersion coefficients depends on the domain size both from the initial sampling of the velocity field and from the average number of correlation lengths crossed by the solute plume. Enlarging the system simultaneously in the x and y directions improves both the initial sampling and the average length of the particle pathlines. The injection window has been fixed as large as possible to optimize the initial velocity sampling. It should not be too large however to avoid particles getting too close to the no-flow sides of the domain where the velocity field is influenced by the presence of the boundary condition [*Englert et al.*, 2006; *Salandin and Fiorotto*, 1998]. We have checked that all particles kept a distance of at least 30 correlation lengths from the no-flow sides of the domain.

[14] We have looked for the smallest domains for which the asymptotic regime is obtained for at least half of the simulation exploitable time range. The exploitable time range extends from the time of injection to the first breakthrough time, that is, the time for which the first particle arrives at the domain outlet. These times strongly depend on σ^2. For the lowest heterogeneity case ($\sigma^2 = 0.25$), a 2048 × 2048 domain ($L_x/dx = L_y/dy = 2048$) with 10 grid cells by correlation length ($\lambda/l_m = 10$) is large enough and long enough to establish the asymptotic regime in the longitudinal direction and for the isotropic local dispersion case ($\alpha_L = \alpha_T$) (Figure 2a). The solute plume reaches the asymptotic regime when its mean position has crossed around 15 correlation lengths ($t_N = 15$). The asymptotic regime is maintained between $t_N = 15$ and $t_N = 150$. For the highest heterogeneity case ($\sigma^2 = 9$), the minimal system sizes for which convergence is maintained over at least half of the time range are $L_x/dx = L_y/dy = 16{,}384$ with 10 grid cells by correlation length ($\lambda/l_m = 10$) (Figure 2b). The asymptotic regime is reached for $t_N = 400$ at the latest and is maintained until the breakthrough time $t_N = 1000$. The exploitable time ranges are comparable with those obtained for the pure advection case (solid curves on Figure 2). System sizes for intermediary σ^2 values are given in Table 1.

[15] Transverse dispersions appear on Figure 3 to be more variable both for the low and high heterogeneity cases. The first reason for the larger variations is the difference in scales over which $D_L(t_N)$ and $D_T(t_N)$ vary. Because of the

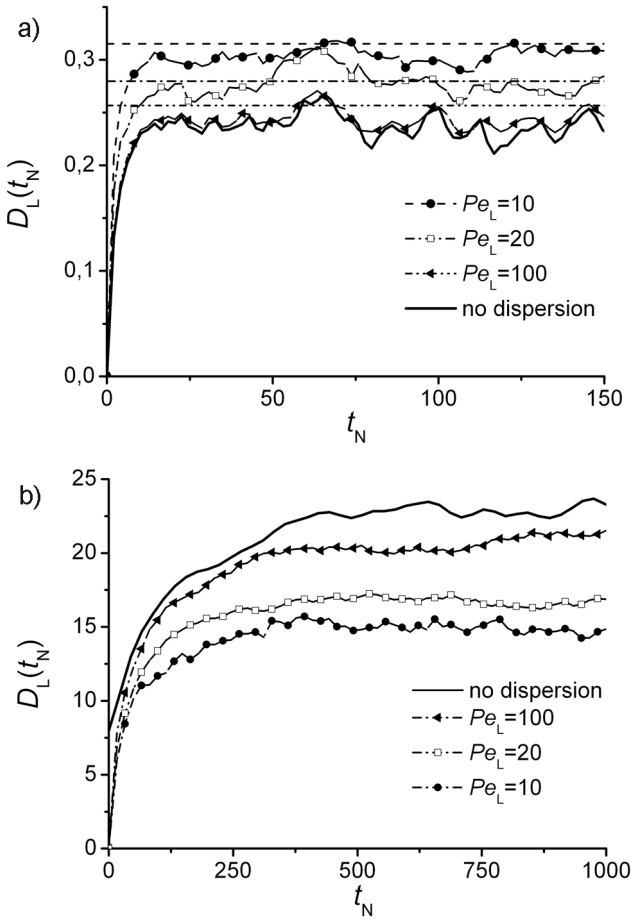

Figure 2. Longitudinal dispersion coefficient normalized by λu as expressed by equation (9) and obtained for isotropic local dispersion $Pe_L = Pe_T$ with (a) $\sigma^2 = 0.25$ and (b) $\sigma^2 = 9$. Results are obtained with $N_p = 5000$ particles and are averaged over $N_S = 100$ simulations. Dashed curves on Figure 2a come from the analytical approximation of *Salandin and Fiorotto* [2000]. Domain sizes are, for $\sigma^2 = 0.25$, $L_x/\lambda = L_y/\lambda = 204.8$ and, for $\sigma^2 = 9$, $L_x/\lambda = 2L_y/\lambda = 1638.4$.

differences in the normalization factors in equations (9) and (10), $D_L(t_N)/D_T(t_N)$ is proportional to Pe_T which ranges between 10 and 100. The second reason is that, because $D_T(t_N)$ is much smaller than $D_L(t_N)$, it is more sensitive to the local velocity variability. Despite its nonmonotonous variations, $D_T(t_N)$ does not show any systematic tendency over the second-half of the exploitable time range.

[16] As, for the domain sizes chosen, the asymptotic regime is maintained over at least the second half of the simulation time range we define the realization-based longitudinal asymptotic dispersion coefficient or macrodispersion coefficient as

$$D_{LA}^i = \frac{\int_{0.5t_b^i}^{t_b^i} D_L^i(t)dt}{t_b^i}, \tag{14}$$

where t_b^i is the first breakthrough time of the ith simulation. The longitudinal macrodispersion coefficient is obtained by averaging over the number of simulations N_S,

$$D_{LA} = \left\langle D_{LA}^i \right\rangle_{i=1,N_s}. \tag{15}$$

The advantage of deriving the asymptotic dispersion coefficient first on a realization basis is to adapt the averaging time range $[0.5t_b^i, t_b^i]$ to the realization first breakthrough time, rather than taking for all simulations the minimum of the realization first breakthrough times t_b. We also determine the variance of $D_L(t)$ over the averaging interval $[0.5t_b, t_b]$ $\sigma(D_{LA})$ and use it as a precision criterion for D_{LA}. From Figure 2, $\sigma(D_{LA})$ represents the amplitude of the variations of $D_L(t)$ on the second half of the simulation time range. The comparison of $\sigma(D_{LA})$ to D_{LA} gives a simple test to determine for which cases the numerical results lead to a reliable estimate of the macrodispersion. Results are significant only when $D_{LA} > \sigma(D_{LA})$. For all asymptotic results presented in this paper $\sigma(D_{LA})/D_{LA}$ and $\sigma(D_{TA})/D_{TA}$ remain always smaller than 0.15. The same procedure is followed to get the transverse dispersion coefficients by replacing index $_L$ by index $_T$. After intensive testing, we have determined that the described methodology can identify macrodispersion for longitudinal and transverse local dispersivities verifying $Pe_L \leq 100$ and $Pe_T \leq 1000$. We recall that the asymptotic coefficients D_{LA} and D_{TA} defined here and used throughout the paper are normalized by λu and $\alpha_T u$. Their definition thus differs from $D_{LA}(GA)$ and $D_{TA}(GA)$ given by equations (3) and (4).

[17] All simulation parameters are recalled in Table 1. The total number of grid cells is equal to $L_x L_y/l_m^2$ and ranges from 4.2×10^6 to 134×10^6 for σ^2 increasing from 0.25 to 9. Simulations $N_S = 100$ are performed for each parameter set and simulations have been performed for 78 parameter sets decomposed in 24 for the convergence with λ/l_m (i.e., 6 values of σ^2 times 4 values of λ/l_m) (A. Beaudoin et al., Convergence analysis of advection diffusion simulations in 2-D heterogeneous porous media, unpublished, 2010) and 54 for the effective determination of the macrodispersion (i.e., 6 values of σ^2 times 3 values of Pe_L times 3 values of Pe_L/Pe_T). All 176 longitudinal and transverse dispersion chronicles have been checked for convergence.

[18] The largest simulations 16,384 × 8192 were performed on a cluster of 1.33 GHz Intel Xeon cores (66 CPUs times 2 cores per CPU) with 4 Gb per CPU. The 8192 × 8192 simulations required only half of the cluster resources and lasted one full day for a single parameter set, corresponding to 100 Monte Carlo simulations. The 2048 × 2048 simulations can be performed on a personal workstation. All

Table 1. Simulation Parameters

Parameter	Values
σ^2	0.25, 1, 2.25, 4, 6.25, 9
Pe_L, Pe_T	10, 20, 100
Pe_L/Pe_T	1, 10, 100
N_S	100
N_p	5000
$[L_x/\lambda, L_y/\lambda]$	[204.8, 204.8] for $\sigma^2 \leq 2.25$ [819.2, 819.2] for $\sigma^2 = 4$ [1638.4, 819.2] for $\sigma^2 > 4$
λ/l_m	2, 5, 10, 20
Injection window	0.4 L_y

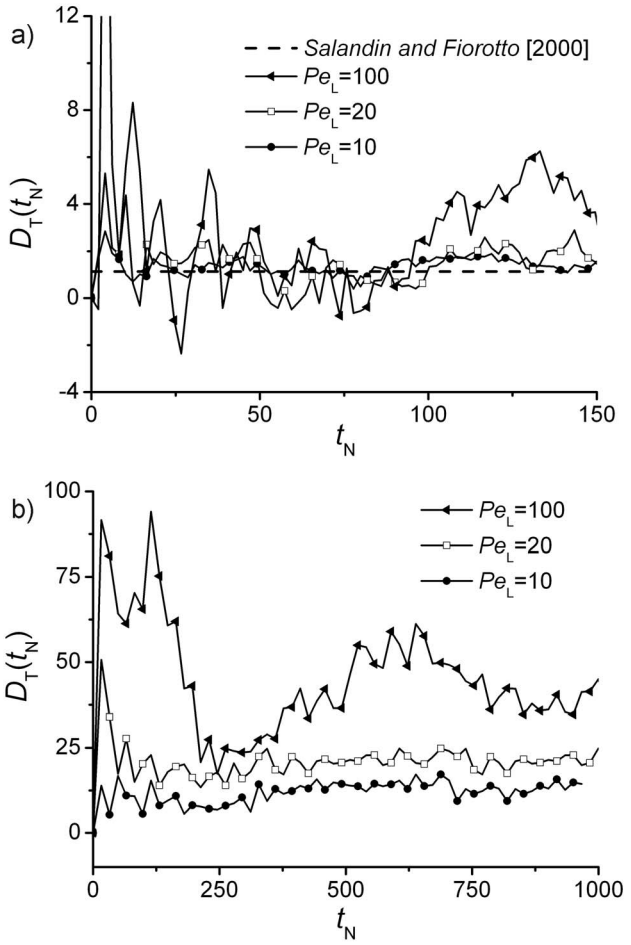

Figure 3. Transverse dispersion coefficient normalized by $\alpha_T u$ as expressed by equation (10) for (a) $\sigma^2 = 0.25$ and (b) $\sigma^2 = 9$. Parameters are identical to those of Figure 2.

taken into account, including the benchmark runs, the simulations required 20 days of computation for the full cluster resources and 50 days for half of the cluster resources. The cumulated single CPU time amounts to 16 years.

4. Results

[19] As our objective is to find the influence of local dispersion on macrodispersion, we use for the longitudinal component the relative difference ΔD_{LA} between the macrodispersion coefficients obtained with local dispersion and with neither dispersion nor diffusion

$$\Delta D_{LA} = [D_{LA}(Pe_L, Pe_T, Pe = \infty)/ D_{LA}(Pe_L = \infty, Pe_T = \infty, Pe = \infty)] - 1. \quad (16)$$

As the transverse macrodispersion in pure advection cases is null [*de Dreuzy et al.*, 2007; *Lunati et al.*, 2002], we keep for the transverse component the quantity D_{TA} given by equation (10). Because of its normalization, D_{TA} can be interpreted as the ratio of the transverse macrodispersion coefficient to the local transverse dispersion coefficient. All values of macrodispersion coefficients given hereafter have been checked for convergence on their corresponding time-dependent dispersion chronicle.

4.1. Isotropic Local Dispersion ($Pe_L = Pe_T$)

[20] We first study the isotropic local dispersion case ($\alpha_L = \alpha_T$) not because of its field relevance but because it can be compared to several existing numerical and analytical results and to results obtained by replacing the local dispersion by the diffusion having on average the same Peclet number. The ΔD_{LA} and D_{TA} display opposite tendencies, as ΔD_{LA} decreases with σ^2 (Figure 4a) while D_{TA} increases with σ^2 (Figure 4b). These tendencies are qualitatively similar to those obtained with theoretical and semianalytical approximation methods [*Neuman et al.*, 1987; *Salandin and Fiorotto*, 2000] and to those obtained with diffusion instead of dispersion [*de Dreuzy et al.*, 2007]. For σ^2 equal to 0.25 and 1, the semianalytical approximation and numerical results of the longitudinal macrodispersion coefficient (filled symbols compared to dashed curves on Figure 4a) are very close together. More precisely the difference is of the order of 4% for $\sigma^2 = 0.25$ and 8% for $\sigma^2 = 1$. The close results of the semianalytical and numerical longitudinal macrodispersion coefficients are a partial a posteriori validation of the numerical methodology. For the transverse macrodispersion, values of D_{TA} for $\sigma^2 = 0.25$ and 1 are at the resolution limit of the numerical methodology and cannot be reliably compared to the analytical approximation.

[21] For $\sigma^2 = 2.25$, the isotropic local dispersion does not induce any discernable effect on the longitudinal macrodispersion coefficient. For $\sigma^2 \geq 4$, the isotropic local dispersion induces a slight reduction of the longitudinal macrodispersion coefficient. The reduction is limited to around 30% at most for $\sigma^2 = 9$ and $Pe_L = Pe_T = 10$. The increase of the transverse macrodispersion coefficient is much more significant as the transverse macrodispersion coefficient is null for pure advection. For σ^2 values larger than 1, the deviation of the semianalytical and numerical results is larger for the transverse macrodispersion coefficient than for the longitudinal macrodispersion coefficient (Figure 4b). The transverse macrodispersion coefficient is specifically triggered by the local dispersion (Figure 4b). The macrodispersion coefficient is, however, 2–50 times larger than the local dispersion ($D_{TA} \in [2, 50]$). The effect of the local dispersion is amplified by the heterogeneity of permeability as D_{TA} increases with σ^2. D_{TA} also increases with less local dispersion (lower Pe_L values). It does not mean that transverse macrodispersion is lower with more local dispersion, but that its amplification is lower with more local dispersion. The amplification is thus linked to the existence of local dispersion or diffusion rather than to their magnitude. The same trends are observed with diffusion instead of dispersion (Figure 4b).

[22] As said previously, the effect of isotropic local dispersion is qualitatively similar to the effect of diffusion. For $\sigma^2 \geq 1$, local dispersion like diffusion induces a reduction of the longitudinal macrodispersion and an increase of the transverse macrodispersion. We have reported on Figure 4 the macrodispersions obtained for diffusion with the same Peclet numbers for local dispersion (Pe_L and Pe_T defined by (6)) and for diffusion (Pe defined by (7)). The objective is to compare more quantitatively the relative effects of diffusion and dispersion. Globally, diffusion induces a reduction of

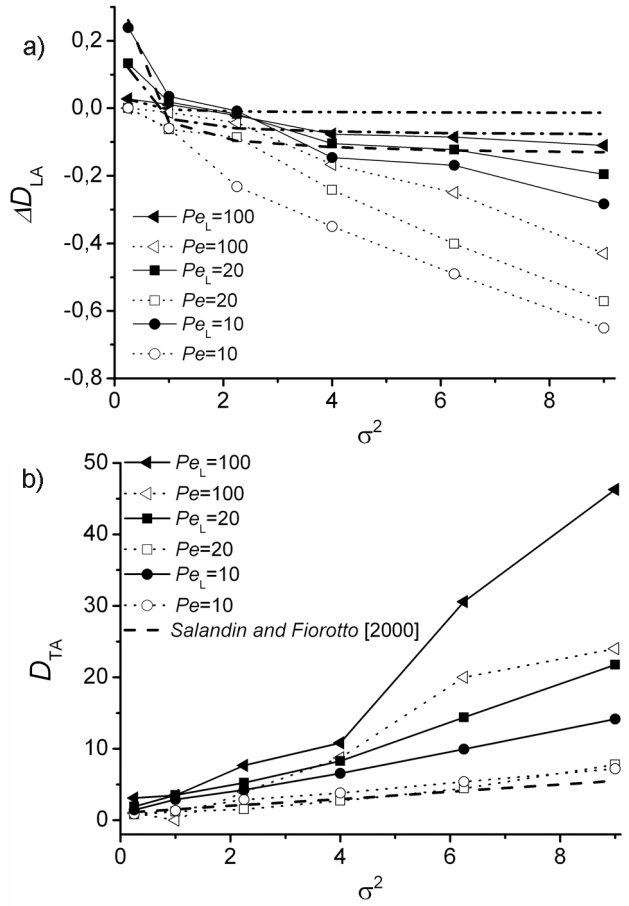

Figure 4. As functions of σ^2 for various values of *Pe* and $Pe_L = Pe_T$: (a) relative difference of longitudinal macrodispersion coefficients and (b) absolute difference of transverse macrodispersion coefficients. Dashed curves come from the analytical approximation of *Salandin and Fiorotto* [2000].

the longitudinal macrodispersion coefficient twice as large as local dispersion. On the contrary the dispersion due to permeability heterogeneities amplifies the transverse local dispersion to the transverse macrodispersion coefficient 1.5–3 times as much as diffusion.

[23] We explain these opposite tendencies by the fact that the local dispersion is larger than diffusion in the high velocity zones whereas diffusion is larger than the local dispersion in the low velocity zones. The longitudinal macrodispersion is especially sensitive to the solutes trapped in the low-velocity zones. Adding diffusion releases them from their trap and significantly reduces the longitudinal macrodispersion coefficient [*de Dreuzy et al.*, 2007]. As local dispersion is proportional to velocity, it is less effective than diffusion as a releasing factor and the reduction of the macrodispersion coefficient is smaller. In the transverse direction, solutes in the high velocity zones are spread laterally further away with dispersion than with diffusion. This could explain the increase of the transverse macrodispersion coefficient.

4.2. Anisotropic Pore-Scale Dispersion ($Pe_L < Pe_T$)

[24] The addition of anisotropy in the local dispersivity does not add much difference to the longitudinal macrodispersion coefficient for values of σ^2 smaller or equal to 2.25 (Figure 5). For σ^2 equal to 0.25, the modification of the longitudinal dispersion coefficient induced by local dispersivity is less than 10% of the global longitudinal macrodispersion coefficient when reducing the transverse dispersion by two orders of magnitude. For σ^2 equal to 1 and 2.25, the longitudinal macrodispersion coefficient is close to 0 for isotropic as well as for anisotropic local dispersion. For σ^2 larger than 2.25, anisotropy lets the longitudinal macrodispersion increase (Figure 5a). The increase is significant at least for the qualitative influence of dispersion. In fact, for high levels of heterogeneities ($\sigma^2 > 1$), the anisotropic local dispersion ($Pe_L/Pe_T \geq 10$) induces an increase of longitudinal macrodispersion coefficient, whereas isotropic local dispersion has the opposite effect, that is, a decrease of the longitudinal macrodispersion coefficient. The same tendencies have been obtained for $Pe_L = 10$ and 100.

[25] In the transverse direction, a decrease of the transverse local dispersion systematically induces a decrease of the transverse macrodispersion coefficient (Figure 5b). From the local scale to the macro scale, the reduction decreases with more permeability heterogeneity. For low-heterogeneity cases ($\sigma^2 \leq 1$), the decrease is of the order of 70% for one order of magnitude decrease of the transverse local dispersion (i.e., from $Pe_L/Pe_T = 1$ to $Pe_L/Pe_T = 10$), the case for which the analytical solution of equation (4) predicts a decrease of 67.5%. For the high-heterogeneity cases ($\sigma^2 > 1$), the reduction of the transverse macrodispersion coefficient is more limited to at most a factor of 2 for a one order of magnitude decrease of the transverse local dispersion.

5. Discussion

[26] Like previous studies [*Gelhar and Axness*, 1983; *Salandin and Fiorotto*, 2000], we find that the contribution of local dispersion to the longitudinal macrodispersion remains highly limited. Quantitatively, the contribution reaches at most 25% for the highest heterogeneity ($\sigma^2 = 9$) but is more generally limited to 10% (Figures 4a and 5a). Qualitatively, local transverse and longitudinal dispersivities induce opposite effects on longitudinal macrodispersion. While the longitudinal dispersivity lets the longitudinal macrodispersion coefficient increase by generating dispersion within the stream tubes, local transverse dispersion lets it decrease by restricting the correlation of velocities along the flow lines [*Matheron and de Marsily*, 1980]. As a result, the longitudinal macrodispersion coefficient either slightly increases for $\sigma^2 \geq 4$ and $Pe_T/Pe_L \geq 10$, does not change for $\sigma^2 = 1$ and 2.25, or slightly decreases in isotropic cases and $\sigma^2 \geq 1$.

[27] The effect of the local dispersion cannot simply be added to the macrodispersion without local dispersion. First, both the longitudinal and transverse local dispersions influence the longitudinal macrodispersion as just said. They also both influence the transverse macrodispersion for $\sigma^2 < 1$ as demonstrated by equation (6)). Second, the transverse macrodispersion is much larger than the local transverse dispersion (Figures 4b and 5b). Most of the amplification factors are in the interval [2, 15] even if they can reach 50. In any case, it is much larger than the predictions of *Salandin and Fiorotto* [2000] (Figure 4b). Third, surprisingly for $\sigma^2 > 1$ the decrease of the transverse local dispersion by two orders of magnitude induces only a reduction of the transverse macrodispersion coefficient by at

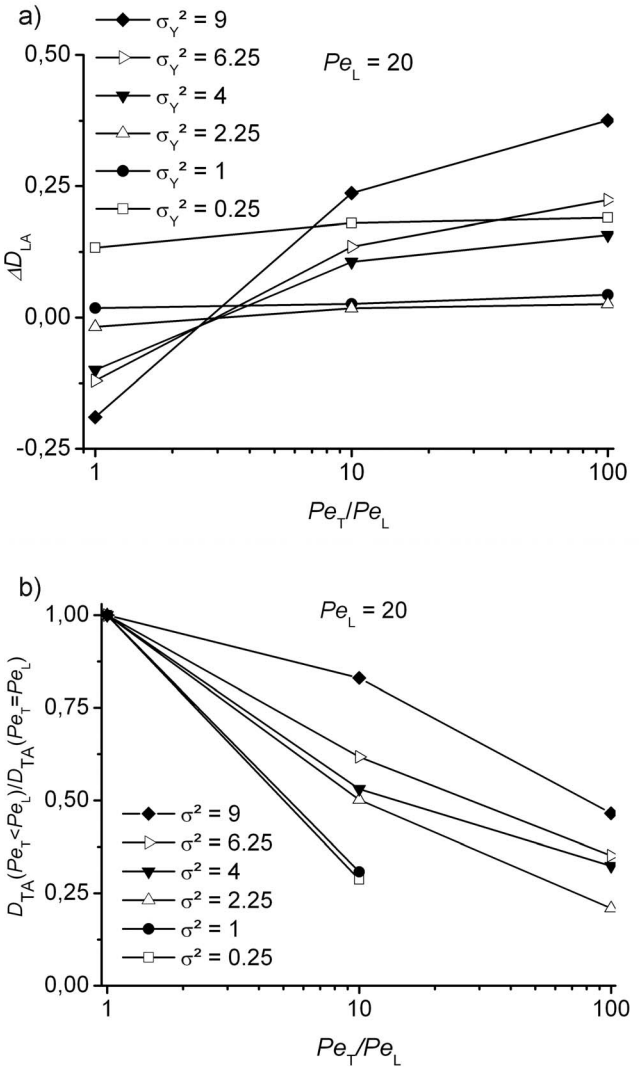

Figure 5. Between the transverse macrodispersion coefficients obtained with anisotropic local dispersion ($Pe_T > Pe_L$) and without isotropic local dispersion ($Pe_L = Pe_T$) as functions of Pe_L/Pe_T for $Pe_L = 20$: (a) ΔD_{LA} and (b) rate. For Figure 5b the transverse macrodispersion coefficient is too small to be measurable with the numerical methodology used in this study, explaining the absence of points for low heterogeneity cases and $Pe_T/Pe_L = 100$.

most a factor of 4 (Figure 5b). The strong tortuosity yielded by the high heterogeneity thus lets the transverse dispersion coefficient strongly increase from the microscale to the macroscale.

[28] Local dispersion is thus critical for the transverse dispersion at least in two dimensions. The transverse macrodispersion only comes from the existence of local dispersion and diffusion. Neglecting the local dispersion would yield a zero transverse macrodispersion coefficient. Adding it simply to the estimates without local dispersion leads to strong underestimates of the transverse macrodispersion. In three dimensions (3D) the situation is different as the estimates of macrodispersion with only advection and neither diffusion nor dispersion give a nonzero transverse dispersion [*Attinger et al.*, 2004; *Dentz et al.*, 2002; *Jankovic et al.*, 2009; *Schwarze et al.*, 2001]. One of the perspectives of this work is to estimate the additional effect of the local dispersion and diffusion in 3D.

6. Conclusions

[29] We have investigated the effect of local-scale dispersion on macrodispersion in heterogeneous 2-D permeability fields. Local-scale dispersion is modeled by longitudinal and transversal dispersivities α_L and α_T. Macrodispersion comes both from the local-scale dispersivities and from the permeability heterogeneity. Permeability has been modeled by a lognormal Gaussian correlated field with a wide range of variances $\sigma^2 \in [0, 9]$. The asymptotic longitudinal and transverse dispersion coefficients have been estimated by using extensive Monte Carlo simulations on large domains. We have determined that the domain sizes necessary for reaching the asymptotic regime ranged from 200 to 1600 correlation lengths λ. We defined the macrodispersion coefficient as the average effective dispersion over a large time interval and on a large enough number of simulations. We have been able to determine macrodispersion only for $\alpha_L/\lambda > 10^{-2}$ and $\alpha_T/\lambda > 10^{-3}$, cases for which the effect of the local dispersion is larger than the precision of the numerically derived macrodispersion. We have found that the effect of the local dispersivities on the longitudinal macrodispersion coefficient remains small whatever the heterogeneity level. Induced modifications are limited to 25% at most of the macrodispersion coefficients due only to permeability heterogeneities. These modifications are smaller than those emerging from the case of a diffusion calibrated to lead to the same values of the Peclet number. The influence on the transverse macrodispersion is much larger as it is null without dispersion and becomes positive with local dispersion. Due to the velocity field heterogeneity, the effect of the local dispersion is amplified by a factor 2 to 50 for $\sigma^2 \geq 2.25$. It is much larger than the effect of a diffusion calibrated to lead to the same values of the Peclet number. On the transverse dispersion, the effect of the dispersion anisotropy remains limited. By reducing by two orders of magnitude the transverse dispersivity with a fixed longitudinal dispersivity, the transverse macrodispersion is reduced only by at most a factor of 4 for $\sigma^2 \geq 2.25$. We conclude that the transverse macrodispersion is triggered by the transverse local dispersion and amplified by the strong stream tube tortuosity emerging from the permeability field heterogeneity.

[30] **Acknowledgments.** The French National Research Agency ANR is acknowledged for its financial founding through the MICAS project (ANR-07-CIS7-004). Numerical computations have been performed on the Grid'5000 experimental test bed, being developed under the INRIA ALADDIN development action. We thank Aldo Fiori for his thoughtful review.

References

Attinger, S., M. Dentz, and W. Kinzelbach (2004), Exact transverse macrodispersion coefficients for transport in heterogeneous porous media, *Stochastic Environ. Res. Risk Assess.*, *18*, 9–15.

Bear, J. (1973), *Dynamics of Fluids in Porous Media*, Dover Publications, Mineola, New York.

Beaudoin, A., J.-R. de Dreuzy, and J. Erhel (2007), An efficient parallel tracker for advection-diffusion simulations in heterogeneous porous media, paper presented at Euro-Par, Rennes, France.

Chaudhuri, A., and M. Sekhar (2005), Analytical solutions for macrodispersion in a 3D heterogeneous porous medium with random hydraulic conductivity and dispersivity, *Transp. Porous Media*, *58*, 217–241, doi:10.1007/s11242-004-6300-8.

Chavent, G., and J. E. Roberts (1991), A unified physical presentation of mixed, mixed hybrid finite elements and standard finite difference approximations for the determination of velocities in waterflow problems, *Adv. Water Resour.*, *14*, 329–348.

de Dreuzy, J.-R., A. Beaudoin, and J. Erhel (2007), Asymptotic dispersion in 2D heterogeneous porous media determined by parallel numerical simulations, *Water Resour. Res.*, *43*, W10439, doi:10.1029/2006WR005394.

de Dreuzy, J.-R., A. Beaudoin, and J. Erhel (2008), Reply to comment by A. Fiori et al. on "Asymptotic dispersion in 2D heterogeneous porous media determined by parallel numerical simulations", *Water Resour. Res.*, *44*, W06604, doi:10.1029/2008WR007010.

Delay, F., P. Ackerer, and C. Danquigny (2005), Solution of solute transport in porous or fractured formations by random walk particle tracking: A review, *Vadose Zone J.*, *4*, 360–379, doi:10.2136/vzj2004.0125.

Dentz, M., and D. M. Tartakovsky (2008), Self-consistent four-point closure for transport in steady random flows, *Phys. Rev. E*, *77*, 066307, doi:10.1103/PhysRevE.77.066307.

Dentz, M., H. Kinzelbach, S. Attinger, and W. Kinzelbach (2000), Temporal behavior of a solute cloud in a heterogeneous porous medium: 1. Point-like injection, *Water Resour. Res.*, *36*, 3591–3604.

Dentz, M., H. Kinzelbach, S. Attinger, and W. Kinzelbach (2002), Temporal behavior of a solute cloud in a heterogeneous porous medium: 3. Numerical simulations, *Water Resour. Res.*, *38*(7), 1118, doi:10.1029/2001WR000436.

Englert, A., J. Vanderborght, and H. Vereecken (2006), Prediction of velocity statistics in three-dimensional multi-Gaussian hydraulic conductivity fields, *Water Resour. Res.*, *42*, W03418, doi:10.1029/2005WR004014.

Erhel, J., J.-R. de Dreuzy, A. Beaudoin, et al. (2009), A parallel scientific software for heterogeneous hydrogeology, *Lect. Notes Comput. Sci. Eng.*, *67*, 39–48, doi:10.1007/978-3-540-92744-0_5.

Falgout, R. D., J. E. Jones, and U. M. Yang (2005), Pursuing scalability for HYPRE's conceptual interfaces, *ACM Trans. Math. Software*, *31*, 326–350.

Fiori, A. (1996), Finite Peclet extensions of Dagan's solutions to transport in anisotropic heterogeneous formations, *Water Resour. Res.*, *32*, 193–198.

Fiori, A. (1998), On the influence of pore-scale dispersion in nonergodic transport in heterogeneous formations, *Transp. Porous Media*, *30*, 57–73.

Fiori, A., G. Dagan, and I. Jankovic (2008), Comment on "Asymptotic dispersion in 2D heterogeneous porous media determined by parallel numerical simulations" by J.-R. de Dreuzy et al., *Water Resour. Res.*, *44*, W06603, doi:10.1029/2007WR006699.

Freeze, R. A. (1975), Stochastic-conceptual analysis of one-dimensional groundwater flow in nonuniform homogeneous media, *Water Resour. Res.*, *11*, 725–741.

Frigo, M., and S. G. Johnson (2005), The design and implementation of FFTW3, *Proc. IEEE*, *93*, 216–231, doi:10.1109/JPROC.2004.840301.

Frippiat, C. C., and A. E. Holeyman (2008), A comparative review of upscaling methods for solute transport in heterogeneous porous media, *J. Hydrol.*, *362*, 150–176, doi:10.1016/j.jhydrol.2008.08.015.

Gelhar, L. W. (1993), *Stochastic Subsurface Hydrology*, Engelwood Cliffs, New Jersey.

Gelhar, L. W., and C. L. Axness (1983), Three-dimensional stochastic analysis of macrodispersion in aquifers, *Water Resour. Res.*, *19*, 161–180.

Gelhar, L. W., C. Welty, and K. R. Rhefeldt (1992), A critical review of data on field-scale dispersion in aquifers, *Water Resour. Res.*, *28*, 1955–1974.

Gutjahr, A. L. (1989), Fast Fourier transforms for random field generation, New Mex. Inst. Min. Technol., Tech Report 4-R58-2690R.

Hoteit, H., R. Mose, A. Younes, F. Lehmann, and Ph. Ackerer (2002), Three-dimensional modeling of mass transfer in porous media using the mixed hybrid finite elements and the random walk methods, *Math. Geol.*, *34*, 435–456.

Jankovic, I., A. Fiori, and G. Dagan (2003), Flow and transport in highly heterogeneous formations: 3. Numerical simulations and comparison with theoretical results, *Water Resour. Res.*, *39*(9), 1270, doi:10.1029/2002WR001721.

Jankovic, I., D. R. Steward, R. J. Barnes, and G. Dagan (2009), Is transverse macrodispersivity in three-dimensional groundwater transport equal to zero? A counterexample, *Water Resour. Res.*, *45*, W08415, doi:10.1029/2009WR007741.

Kitanidis, P. K. (1988), Prediction by the method of moments of transport in a heterogeneous formation, *J. Hydrol.*, *102*, 453–473.

La Bolle, E. M., G. E. Fogg, and A. F. B. Thompson (1996), Random-walk simulation of transport in heterogeneous porous media: Local mass-conservation problem and implementation methods, *Water Resour. Res.*, *32*, 583–593.

Lunati, I., S. Attinger, and W. Kinzelbach (2002), Macrodispersivity for transport in arbitrary nonuniform flow fields: Asymptotic and preasymptotic results, *Water Resour. Res.*, *38*(10), 1187, doi:10.1029/2001WR001203.

Matheron, G., and G. de Marsily (1980), Is transport in porous media always diffusive? A counterexample, *Water Resour. Res.*, *16*, 901–917.

Neuman, S., C. Winter, and C. Newman (1987), Stochastic-theory of field-scale fickian dispersion in anisotropic porous media, *Water Resour. Res.*, *23*, 453–466.

Pardo-Igúzquiza, E., and M. Chica-Olmo (1993), The Fourier integral method: an efficient spectral method for simulation of random fields, *Math. Geol.*, *25*, 177–217, doi:10.1007/BF00893272.

Pollock, D. W. (1988), Semianalytical computation of path lines for finite-difference models, *Ground Water*, *26*, 743–750.

Ramirez, J. M., E. A. Thomann, E. C. Waymire, J. Chastanet, and B. D. Wood (2008), A note on the theoretical foundations of particle tracking methods in heterogeneous porous media, *Water Resour. Res.*, *44*, W01501, doi:10.1029/2007WR005914.

Salamon, P., D. Fernandez-Garcia, and J. J. Gomez-Hernandez (2006), A review and numerical assessment of the random walk particle tracking method, *J. Contam. Hydrol.*, *87*, 277–305.

Salandin, P., and V. Fiorotto (1998), Solute transport in highly heterogeneous aquifers, *Water Resour. Res.*, *34*, 949–961.

Salandin, P., and V. Fiorotto (2000), Dispersion tensor evaluation in heterogeneous media for finite Peclet values, *Water Resour. Res.*, *36*, 1449–1455.

Schwarze, H., U. Jaekel, and H. Vereecken (2001), Estimation of macrodispersion by different approximation methods for flow and transport in randomly heterogeneous media, *Transp. Porous Media*, *43*, 265–287.

Trefry, M. G., F. P. Ruan, and D. McLaughlin (2003), Numerical simulations of preasymptotic transport in heterogeneous porous media: Departures from the Gaussian limit, *Water Resour. Res.*, *39*(3), 1063, doi:10.1029/2001WR001101.

Uffink, G. J. M. (1985), A random walk method for the simulation of macrodispersion in a stratified aquifer, *IAHS Publ.*, *146*, 103–114.

van Kampen, N. G. (1981), *Stochastic Processes in Physics and Chemistry*, Elsevier Sci., Amsterdam.

A. Beaudoin, Institut P′, UPR 3346 CNRS, Université de Poitiers, ENSMA, SP2MI, Téléport 2, Boulevard Marie et Pierre Curie, BP 30179, Futuroscope, F-86962 Chasseneuil CEDEX, France. (anthony.beaudoin@univ-poitiers.fr)

J.-R. de Dreuzy, Géosciences de Rennes, UMR 6118 CNRS, Université de Rennes 1, Campus de Beaulieu, Bâtiment 15, F-35042 Rennes CEDEX, France.

J. Erhel, INRIA Rennes, Campus de Beaulieu, Avenue du Général Leclerc, F-35042, Rennes CEDEX, France.